

NMR DIFFUSION EDITING FOR D - T_2 MAPS: APPLICATION TO RECOGNITION OF WETTABILITY CHANGE

M. Flaum, J. Chen, and G. J. Hirasaki, Rice University

ABSTRACT

The inclusion of diffusion information in addition to relaxation is making a significant contribution to the interpretation of NMR well logs. The results can be displayed as a 2-D map or distribution of diffusion coefficient versus relaxation time, called $D - T_2$ maps. These maps have already been proven useful as tools for fluid characterization and probes of restricted volumes, but there are other benefits to employing 2-D maps for interpretation. Divergence of the measured diffusion coefficient from bulk fluid values can give information about the system in which diffusion is occurring. For example, diffusion coefficient values above the bulk fluid diffusivity indicate the presence of internal field gradients, while values below bulk suggest the presence of restricted diffusion. Diffusion information can also indicate wettability alteration. When an oil phase relaxes and diffuses as bulk oil, the response will appear on the line corresponding to the correlation of diffusivity and relaxation time for hydrocarbons. Departure of the oil response from this line to shorter relaxation time is usually due to surface relaxation of the oil phase, indicating a change in wettability. This change can also be indicated by the water phase relaxation time shifting towards the bulk value, a phenomenon more easily monitored when oil saturations are low.

The naturally oil-wet character of West Texas dolomites, as well as the wettability alteration due to oil-based drilling mud additives in Berea sandstones was interpreted by diffusion editing. In addition to the interpretation detailed above, the separation of water and oil components allows the monitoring of changes in the water bound volume irreducible when wettability changes occur. In these samples, the interpretation must be qualified with the condition that internal gradients will also result in departure of the oil response from the line for hydrocarbons. These examples will illustrate the

process of generating and interpreting $D - T_2$ maps to observe internal gradients, multiple fluid saturations, and wettability changes.

INTRODUCTION

Supplementing standard relaxation time measurements with diffusion information provides a wealth of new interpretation for NMR well logs. Rather than observing response in the presence or absence of diffusion, the results can be displayed as a 2-D map or distribution of diffusivity versus relaxation time, called $D - T_2$ maps (Hurlimann and Venkataramanan, 2002). These maps provide a clear and visual approach to the extra interpretation available with the inclusion of diffusion information.

The use of $D - T_2$ maps to determine saturations through fluid separation has been established in recent research (Hurlimann *et al.*, 2002; Hurlimann *et al.*, 2003). Diffusion information can contribute to interpretation in a number of other ways as well, largely through monitoring the divergence of the measured diffusion coefficient from the bulk self-diffusion constant of the fluid. For example, diffusion coefficient values above the bulk fluid diffusivity indicate the presence of internal field gradients (Sun and Dunn, 2002; Hurlimann *et al.*, 2003), while values below bulk suggest the presence of restricted diffusion. Diffusion data can also indicate wettability alteration (Freedman *et al.*, 2002). When an oil phase relaxes and diffuses as bulk oil, the response will appear on the line corresponding to the correlation of diffusivity and relaxation time for hydrocarbons. Departure of the oil response from this line to shorter relaxation time is usually due to surface relaxation of the oil phase, indicating a change in wettability. This change can also be indicated by the water phase relaxation time shifting towards the bulk value.

One technique for obtaining diffusion and relaxation information simultaneously is

called Diffusion Editing (DE), where the sample signal is “edited” by allowing diffusion to occur before relaxation data is collected (Hurlimann and Venkataraman, 2002). By collecting a series of measurements with varying diffusion times, the diffusion coefficient of the sample is evaluated from the amplitude of the remaining signal. Relaxation time is obtained by monitoring the decay of that signal through a series of spin echoes, similar to a Carr-Purcell-Meiboom-Gill pulse sequence. The resulting matrix for each diffusion time and echo time can be inverted through algorithms such as described by Venkataraman *et al.* (2002) to obtain a $D - T_2$ map.

The version of DE employed here is based on a modification of the standard gradient CPMG measurement, with the echo spacings of the first two echoes extended to provide the diffusion time. The selection of diffusion times to complete the data suite determines the range and resolution of the resulting $D - T_2$ map, and thus must be tailored to fit the system at hand. Furthermore, some regions of $D - T_2$ space cannot be characterized correctly, as a balance must exist between signal loss due to relaxation and due to diffusion. If too much signal is lost due to relaxation before diffusion affects the signal amplitude at all, it will not be possible to characterize the diffusivity of those components of the system. The selection of the applied magnetic field gradient effects this region, though in most oilfield applications, the applied magnetic field gradient is constrained by the instrumentation at hand. In many cases it is necessary to indicate regions of poor diffusivity information instead of attempting to tailor the gradient to maximize the regions of available information.

In this document, the methodology for employing DE measurements to obtain $D - T_2$ is presented, and applied to the problem of monitoring wettability changes in a variety of rock samples. The naturally oil-wet character of West Texas dolomites, as well as the wettability alteration due to oil-based drilling mud additives in Berea sandstones was interpreted by diffusion editing. In addition to the interpretation detailed above, the separation of water and oil

components allows the monitoring of changes in the water bound volume irreducible when wettability changes occur. In these samples, the interpretation must be qualified with the condition that internal gradients will also result in departure of the oil response from the line for hydrocarbons. These examples will illustrate the process of generating and interpreting $D - T_2$ maps to observe internal gradients, multiple fluid saturations, and wettability changes.

DIFFUSION EDITING MEASUREMENTS

The CPMG-DE measurement consists of a suite of similar NMR measurements (Hurlimann *et al.* 2002). The sequence is displayed in Fig. 1. The independent variable that provides diffusion information is the echo spacing of the first two echoes of the sequence (called $T_{E,L}$). An increase in the spacing of these two echoes decreases the amplitude of subsequent echoes due to diffusion effects. The remaining echoes are at a fixed shorter echo spacing ($T_{E,S}$) selected to minimize further relaxation due to diffusion. The progressive amplitude loss over the first two echoes for a series of $T_{E,L}$ values provides information about the diffusivity of fluids in the sample, while the multi-exponential decay of subsequent data points provides T_2 relaxation distributions.

The equation describing the magnetization decay of a CPMG DE sequence is shown in Eq. 1 (Hurlimann *et al.*, 2002). Note that the diffusion and relaxation terms are separable. The off-resonance (stimulated) echo contributions can be quite significant and the stimulated echoes decay under diffusion at twice the rate of the direct echo (Hurlimann *et al.* 2002). The contribution from the off-resonance terms can be included as a second diffusion term, as in Eq 1. a and b are attenuation coefficients dependent on bandwidth. a represents the contribution from the direct echo, and b represents the contribution from the stimulated echo. The values of a and b can be determined by performing a least-squares fit on a sample of known diffusivity, such as a water bottle at controlled temperature.

Like any fixed-gradient measurement,

$$M(t_{E,L}, t) = \iint dDdT_2 f(D, T_2) e^{-t/T_2} \left[a \exp\left\{-\frac{1}{6} \gamma^2 g^2 D t_{E,L}^3\right\} + b \exp\left\{-\frac{1}{3} \gamma^2 g^2 D t_{E,L}^3\right\} \right] \quad (1)$$

the CPMG DE only measures a thin slice of the total sample, corresponding to the bandwidth of the hardware. To best characterize the echoes collected for these experiments, a matched filter can be employed. In the matched filter technique, multiple points must be collected for each echo, enough to characterize the full shape of the echo without adding extraneous noise to the signal. A mean echo shape for each channel is obtained by averaging a segment of echoes of the shortest $T_{E,L}$ data set where $T_{E,L}$ is not equal to $T_{E,S}$. The segment should not include the first two echoes, where spin dynamic effects distort the echo shape (Hurlimann, 2001), nor should they include any subsequent echoes that indicate oscillation or phase drift. The average echo is then used as a windowing filter for all the subsequent echoes, using a dot product with the real echoes of all data sets to obtain a single value for each echo of each channel of all data sets.

The selection of the diffusion time list ($T_{E,L}$) determines the range and resolution of the $D - T_2$ map that can be obtained from the data suite. It is useful to include one $T_{E,L}$ equal to the $T_{E,S}$, to provide a basic CPMG measurement in the data suite. The remainder of the list should be determined based on the expected range of diffusion coefficients of the sample. The attenuation expected for a given diffusion coefficient can be predicted using the diffusion kernel from Eq. 1. If there is no hydrocarbon present, very long diffusion times are unnecessary, and it may be beneficial to include very short diffusion times to watch for evidence of internal gradients (diffusion coefficients above that of bulk water). When crude oils or other slow-diffusing components are present, the longest diffusion time should be long enough to fully attenuate a sample with diffusion coefficients below 1×10^{-6} cm²/s, and possibly longer if very heavy oil is expected. For the experiments performed in this study, the $T_{E,L}$ list was selected by choosing 10 diffusion times that would provide a range of attenuation values, including minimal attenuation and complete attenuation for samples diffusing both at 2.25×10^{-5} cm²/s (bulk water value) and 1×10^{-6} cm²/s. It should be noted that minimal attenuation is not zero, as the sum of pre-exponential factors a and b from Eq. 1 is less than 1.

$D - T_2$ MAPS

A sample $D - T_2$ map based on CPMG-DE measurements is shown in Fig. 2. The map is a contour plot with diffusion coefficient on the Y axis and relaxation on the X axis. This particular map shows the results for simulated data, with the actual values of D and T_2 marked with black circles (for simulated data only). There are several other details indicated on this map that will not be labeled on further examples, so it will be useful to discuss their necessity here. The horizontal dashed line indicated the self-diffusion coefficient of bulk water at the experimental conditions. The solid diagonal line with a positive slope, on the right-hand side of the diagram, indicates the correlation between diffusivity and T_2 for hydrocarbon mixtures according to Lo et al (2002).

On the left-hand side, there are three other diagonal lines, each with the same negative slope. These lines indicate the region where diffusion information becomes progressively sparser. They are plotted using the X axis as diffusion time (t_D) in place of relaxation time, and delineate the trade-off between relaxation based and diffusion based attenuation. Both diffusion and relaxation are measured through signal attenuation, and it is important to have adequate attenuation due to diffusion before too much the signal attenuates due to relaxation. The rightmost line indicating the time where the attenuation due to diffusion at that t_D will be 50% of the remaining signal, the middle line 20%, and the leftmost line showing where only 5% of the total signal will be attenuated due to diffusion. These lines indicate the range where relaxation strongly dominates signal attenuation, and thus indicate the limits of where diffusion measurements will be possible. Any component with a diffusion and relaxation pairing that falls to the left of these lines will have attenuated due to relaxation to the point where any attenuation due to diffusion would be negligible. These lines act as a guideline for the interpreter, showing that any information to the left of these lines is artifact, and any results falling on the lines is unreliable. These lines will be referred to later in this document as the diffusion limit lines.

The diffusion limit lines are necessary to prevent over-interpretation of areas of the $D - T_2$ map that do not contain reliable information. There are a number of algorithms for inverting the DE data suites, and each treat short-relaxing,

slow diffusing components differently. The algorithm employed for the results in this work requires that the data exists as a complete matrix, with magnitude information at every echo time for every data set. As originally written it did not take into account any relaxation information from data points shorter than the third echo of the longest $T_{E,L}$ because each data set lacks equally-spaced echoes during the diffusion time. That means if $T_{E,L}$ must be long for correct diffusion characterization, short T_2 information will be lost. It is necessary to trade off low-diffusion coefficient information for short relaxation information, or vice versa. To avoid this problem, it is necessary to work with data sets that have information for each data set at the echo times corresponding to the basic CPMG measurement. Since it is not possible to acquire results during the diffusion time, these times must instead be filled with data extrapolated from the available information.

The extrapolation is performed in two steps. First, each data set in the suite is inverted through standard T_2 fitting algorithms to obtain relaxation time distributions. These distributions are then used to provide evenly spaced fitted echo data for the times missing from the data set. The extrapolated data should contain no relaxation or diffusion information that was not present in the measured data, but there is now echo information for each data set at each echo time, so the entire set can be inverted using the same basic algorithm without truncating the data at all. Some artifacts will occur due to regularization error, but careful avoiding over-regularization should minimize the detrimental effects of these artifacts.

Fig. 3 shows the $D - T_2$ map of a Bentheim sandstone sample fully saturated with brine. There is a single peak visible in the plot, with a diffusion coefficient distribution centered at 2.00×10^{-5} cm²/s and a T_2 range between 200 milliseconds and 1.2 seconds. The diffusion coefficient value indicated suggests that all of the water in the sample diffuses close to bulk, with little restricted diffusion occurring. Fig. 4 shows again the Bentheim sample, this time with an oil saturation of approximately 57%. Here, one peak corresponding to the water content is clearly visible, as well as another representing the oil. The oil peak is very much the same as it appeared at higher saturations, again behaving as bulk oil. The water peak still diffuses as it did in the fully water-saturated measurement, but the T_2

distribution has lost all amplitude above 1 second. This indicates that the largest pores, formerly occupied by water, have been filled with oil instead, and the water is now contained in smaller, faster relaxing pores. The water still lines the walls of the larger pores (otherwise the oil T_2 distribution would be affected by oil wetting) but the reduced volume of water present increases the surface/volume ratio, and thus decreases relaxation time.

When only a single fluid is present, interpretation is based on diffusion coefficient values moving away from the bulk value for the fluid. One circumstance in which this can occur is referred to as restricted diffusion. Restricted diffusion occurs when spins are not able to displace as far as they should, due to confinement in an enclosed space such as a pore. The measured diffusion coefficient when spins undergo restricted diffusion is lower than the bulk diffusivity of the fluid. An example of restricted diffusion in a $D - T_2$ map is shown in Fig. 5. Most of the signal for the 40 mD carbonate sample shown appears to have a diffusion coefficient below that of bulk water. The presence of restricted diffusion at relatively long relaxation times indicates the sample has a low relaxivity, as anticipated in carbonate samples.

The measured diffusion coefficient of a sample can also appear above the bulk diffusivity of the fluid present. This occurs when internal field gradients are present in the sample, due to iron-containing clays or other minerals. An example of a 100 mD Berea sandstone with internal field gradients is shown in Fig. 6. The bulk of the signal continues to diffuse as bulk water, but a strong peak well above the diffusivity of water is also visible, extending to the shortest relaxation times present. This indicates that internal field gradients are a major factor in the smaller pores, but not all spins in the system experience an internal field gradient.

WETTABILITY ALTERATION

Obtaining wettability information through NMR is of use for predicting oil production, evaluating invasion of oil-based mud filtrates, and estimating oil viscosity. Surface relaxation occurs in any phase in contact with the pore walls, so if a sample becomes oil-wet, the relaxation time of the oil sample should be shorter than that of the bulk oil due to surface

relaxation of the oil. The water phase of an oil-wet sample relaxes correspondingly slower, as the contact area between water and the surface is reduced. In many situations, however, overlap between the relaxation distributions of the various phases makes it impossible to monitor changes in the individual distributions of separate phases. Obtaining separate distributions for the separate phases removes ambiguity and allows direct evaluation of any changes in the wettability of the sample.

The relaxation time distributions of the same 40 mD carbonate sample at 100% brine saturation and at high oil saturation are shown in Fig. 7. The brine-saturated sample has a maximum relaxation time of about 1.5 seconds, and a peak around 600 milliseconds. When a 19 cp crude oil is present, the long relaxation time portion of the distribution stretches out as far as 2 seconds, and the peak position of the sample dropped to around 100 milliseconds. Without any information about the bulk properties of the crude oil present, it would be assumed that both changes in the distribution were due to the addition of crude oil components, implying that the crude oil contains components that relax slower than 1.5 seconds as well as components that relax faster than 600 milliseconds.

With the addition of $D - T_2$ maps to provide separate fluid distributions, it is possible to obtain a more complete picture of the situation. The map of the fully water-saturated sample is shown in Fig. 5. The bulk of the distribution lies below the bulk diffusion coefficient of water, indicated the presence of restricted diffusion. The same system with crude oil added is shown in Fig. 8. The oil contribution falls cleanly along the correlation line until it reaches the diffusion limit, with basically no components over 1 second. The slow-relaxing portion is clearly attached to the brine portion of the distribution, indicating that the brine is relaxing slower than it did in the fully brine-saturated sample. This transition indicates a change in the wettability of the sample. The brine component is no longer in contact with the surface of the sample in all pores, so the degree of surface relaxation of the water has decreased. This can be confirmed by comparing the distribution of the bulk oil to a projection of the oil portion of the $D - T_2$ map. Fig. 9 shows that comparison. Shift of the distribution to shorter relaxation time confirms

the wettability change implied by changes in the brine distribution.

The second example presented here involves a more complicated picture. Two samples of Berea sandstone were partially saturated with SB base oil, with the base oil in one case containing some surfactant additives found in standard drilling muds. The objective was to determine if the inclusion of surfactant additives changed the wettability of the sandstone, usually a strongly water-wet rock. Relaxation time distributions for the samples are shown in Fig. 10. In both partially-saturated samples, the distributions now include a peak relaxing longer than the original brine-saturated distribution. The bulk base oil is also shown on the same plot, suggesting that in both cases, this slow relaxing peak is due to the bulk relaxation of base oil. It is not possible to distinguish any wettability differences between the two samples from these distributions.

The $D - T_2$ map for the brine-saturated sample is shown in Fig. 6. The relaxation times are all less than one second, and the diffusion coefficient is largely centered around the value for bulk water, but contains some significantly higher values, indicating the presence of internal field gradients. This sample is entirely water-wet, as there is no hydrocarbon present to wet the surface.

The $D - T_2$ map for the partially base oil-saturated sample without additive is shown in Fig. 11. The oil and water portions of the distribution are not clearly separated, due to limited resolution and the proximity of their respective relaxation and diffusion coefficient distributions. Still, it is possible to obtain approximate relaxation distributions by dividing the map at a cutoff diffusion coefficient decided either by inspection, or at a value based on the bulk diffusivity of the base oil. A $D - T_2$ map for the base oil is shown in Fig. 12, showing the maximum of the diffusivity distribution is around $8 \times 10^{-6} \text{ cm}^2/\text{s}$, which can be used as the rough cut-off for the partially saturated sample. The resulting oil and brine distributions are shown in Fig. 13 for the water, and Fig. 14 for the oil. The oil distribution is close to the relaxation time distribution for the bulk oil relaxation time distribution, excluding short-time peaks that are probably either artifact or water undergoing restricted diffusion. The brine T_2 distribution in the absence of additives overlaps the dominant peak of the fully brine-saturated

sample. This latter fact in particular strongly suggests that this sample has remained water-wet in the presence of base oil without additives.

The $D - T_2$ map for the partially base-oil saturated sample including 3% NOVA surfactant additives is shown in Fig. 15. Again, the distributions from the individual fluids are not easily identified, and the cutoff based on the bulk oil diffusivity was employed to distinguish oil and water. The T_2 distributions obtained are also included in Fig. 13 for the brine portion and Fig. 14 for oil. The oil distribution is largely in agreement with the bulk sample, and in fact nearly overlays the distribution for the sample without additive. The water distribution, on the other hand, has shifted considerably towards longer relaxation times, indicating a change in the wettability of the sample to a partially oil-wet system. The surfactant additive has successfully changed the wettability of the system, and the effect would not be observable through standard NMR observation.

CONCLUSIONS

New measurements that take advantage of the presence of magnetic field gradients present in most NMR logging tools have already provided useful information unavailable through more traditional measurements. New interpretations for the diffusivity of rock samples, along with new applications for separated individual fluid relaxation distributions available through the use of $D - T_2$ maps, continue to improve the range of information available from NMR logs.

The first benefit of the $D - T_2$ maps is that the response of oil and water can be distinguished by diffusion editing even when relaxation time distributions overlap.

The second benefit presented in this work is the identification of wettability alteration from water-wet conditions by comparing the oil T_2 distribution with that of bulk oil and comparing the water T_2 distribution with that of 100% water-saturated condition.

REFERENCES

Freedman, R. *et al.*: "Wettability, saturation, and viscosity using NMR measurements" SPEJ (Dec. 2003), 317-324

Hurlimann, M. D.: "Diffusion and relaxation in general stray field NMR experiments" *Journal of Magnetic Resonance*, **148**, (2001), 367-378

Hurlimann, M. D., and Venkataramanan, L.: "Quantitative measurement of two-dimensional distribution functions of diffusion and relaxation in grossly inhomogeneous fields," *Journal of Magnetic Resonance*, **157**, (2002), 31-42

Hurlimann M. D. *et al.*: "Diffusion-editing: new NMR measurement of saturation and pore geometry," paper FFF presented at the 2002 Annual Meeting of the Society of Professional Well Log Analysts, Oiso, Japan, June 2-5 2002.

Hurlimann, M. D. *et al.*: "Diffusion-relaxation distribution functions of sedimentary rocks in different saturation states," *Magnetic Resonance Imaging*, **21**, (2003), 305-310

Hurlimann, M. D. *et al.*: "Application of NMR diffusion editing as a chlorite indicator," paper SCA2003-26 presented at the International Symposium of the Society of Core Analysts held in Pau, France, 21-24 September 2003

Lo, S.-W. *et al.*: "Mixing rules and correlations of NMR relaxation time with viscosity, diffusivity, and gas/oil ratio of methane/hydrocarbon Mixtures," *SPE Journal* (March 2002), 24-34

Sun, B, and Dunn, K.-J.: "Probing internal field gradients of porous media," *Physical Review E*, **65** (2002), 1-7

Venkataramanan, L., Song, Y.Q., Hurlimann, M. D.: "Solving fredholm integrals of the first kind with tensor product structure in 2 and 2.5 dimensions," *IEEE Transactions on Signal Processing*, **50**, No. 5 (2002), 1017-1026

AUTHORS

Mark Flaum received a BEng in Chemical Engineering from McGill University, and is currently pursuing a doctorate at the Chemical Engineering Department of Rice University. His research focuses on the use of NMR diffusion-based measurements for characterization of porous media.

Jiansheng Chen currently is a Ph.D. candidate in the chemical engineering department at Rice University. His thesis work is on NMR surface relaxation, wettability and oil base mud drilling fluids under the direction of Dr. George J. Hirasaki. He can be reached at jschen@rice.edu.

George J. Hirasaki

B.S. Chemical Engineering (1963) Lamar University

Ph.D. Chemical Engineering (1967) Rice University

George had a 26-year career with Shell Development and Shell Oil Companies before joining the Chemical Engineering faculty at Rice University in 1993. At Shell, his research areas were reservoir simulation, enhanced oil recovery, and formation evaluation. At Rice, his research interests are in NMR well logging, reservoir wettability, enhanced oil recovery, gas hydrate recovery, asphaltene deposition, emulsion coalescence, and surfactant/foam aquifer remediation. He received the SPE Lester Uren Award in 1989. He was named an Improved Oil Recovery Pioneer at the 1998 SPE/DOR IOR Symposium. He was the 1999 recipient of the Society of Core Analysts Technical Achievement Award. He is a member of the National Academy of Engineers.

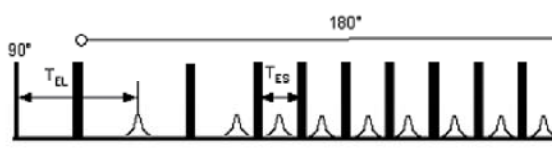


Figure 1: CPMG-DE Pulse Sequence

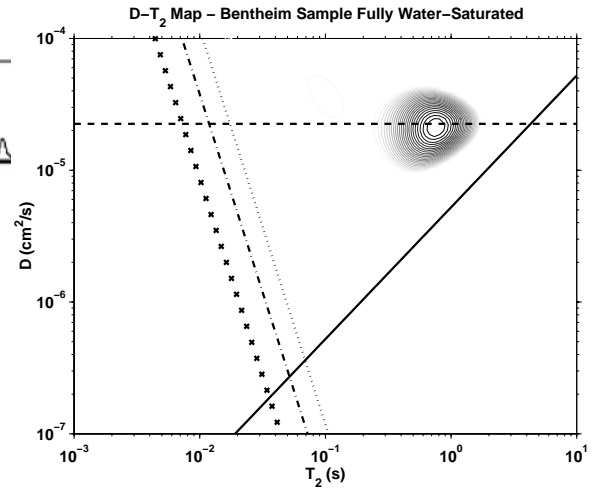


Figure 3: Bentheim Sandstone $D - T_2$ Map, Fully Brine-Saturated

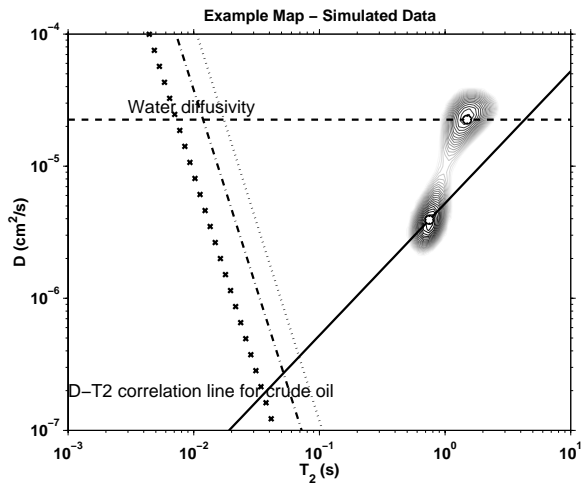


Figure 2: Sample $D - T_2$ Map with Simulated Data

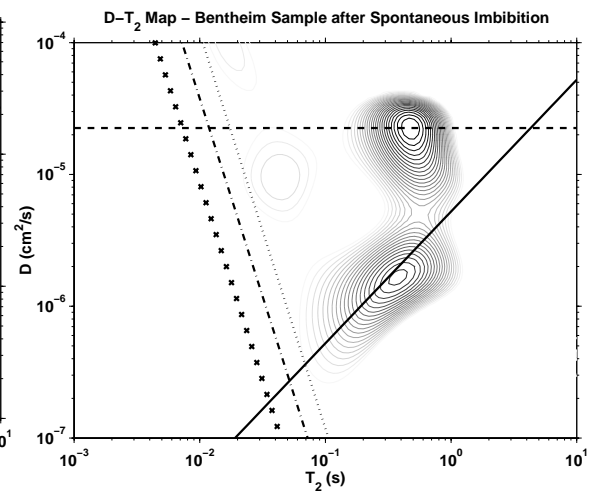


Figure 4: Bentheim Sandstone $D - T_2$ Map, Partially Oil-Saturated

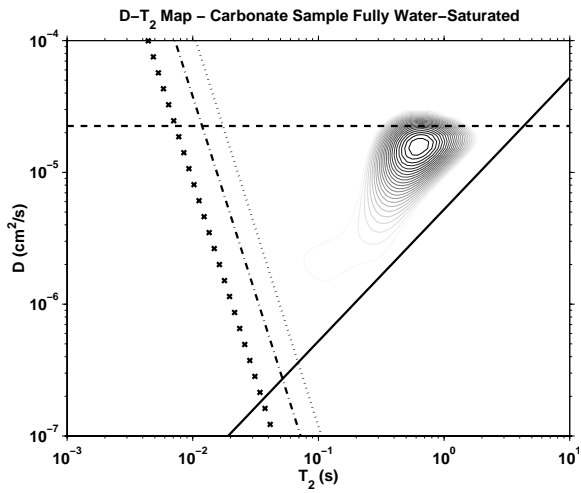


Figure 5: Carbonate Sample $D - T_2$ Map, Fully Brine-Saturated

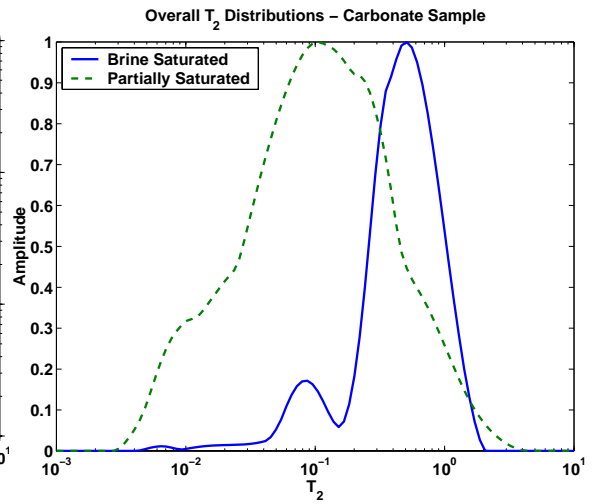


Figure 7: Relaxation Time Distributions for Carbonate Sample

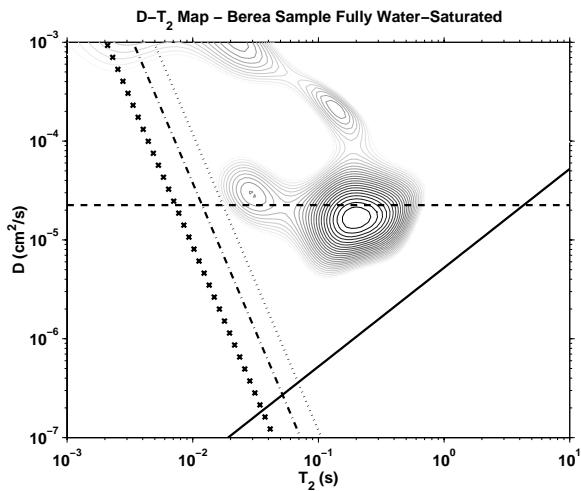


Figure 6: Berea Sandstone $D - T_2$ Map, Fully Brine-Saturated

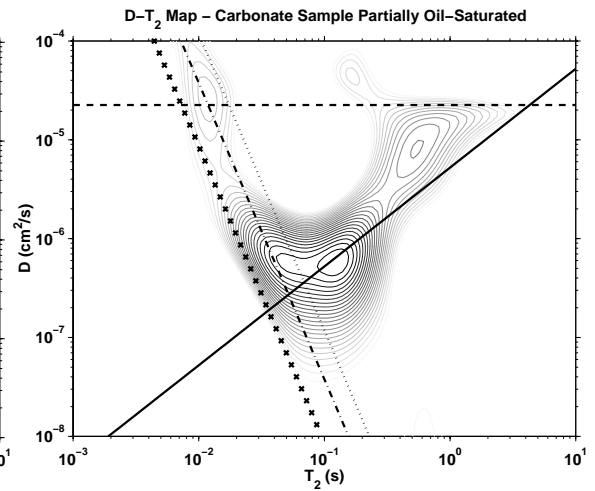


Figure 8: Carbonate Sample $D - T_2$ Map, Partially Oil-Saturated

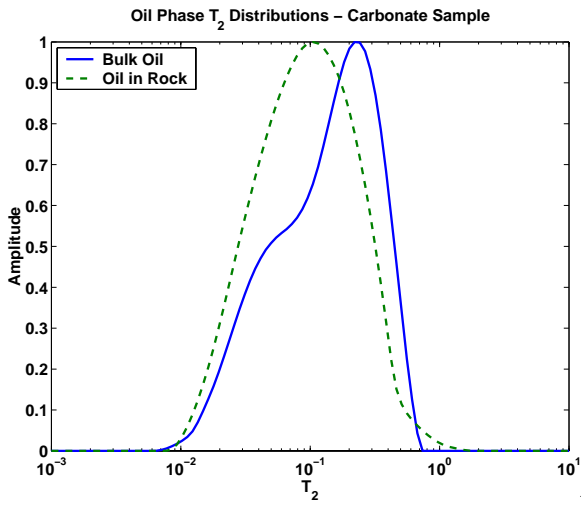


Figure 9: Relaxation Time Distribution For Crude Oil in Carbonate

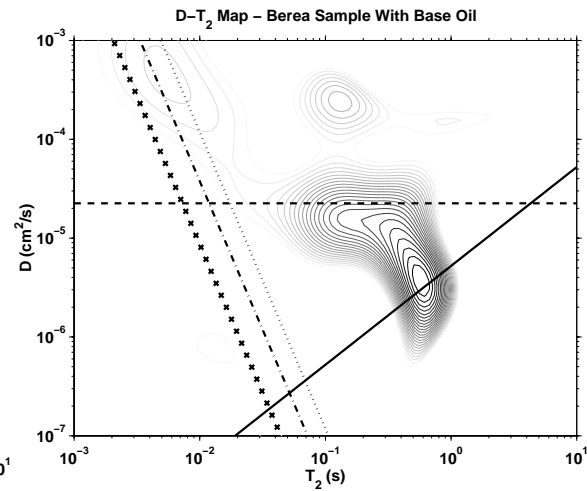


Figure 11: Berea Sandstone $D - T_2$ Map, Partially Saturated With Base Oil, No Additives

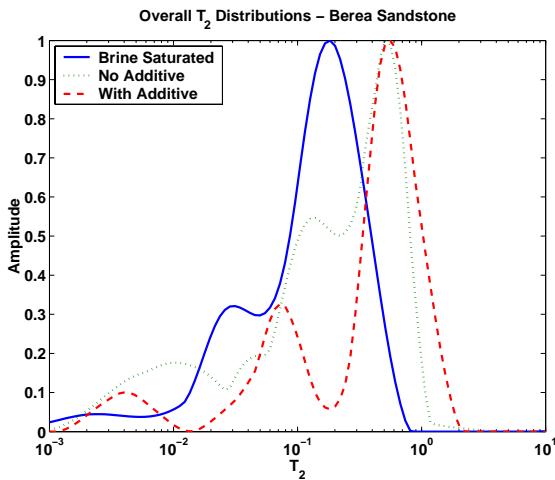


Figure 10: Relaxation Time Distributions for Berea Sandstone at Three Saturations

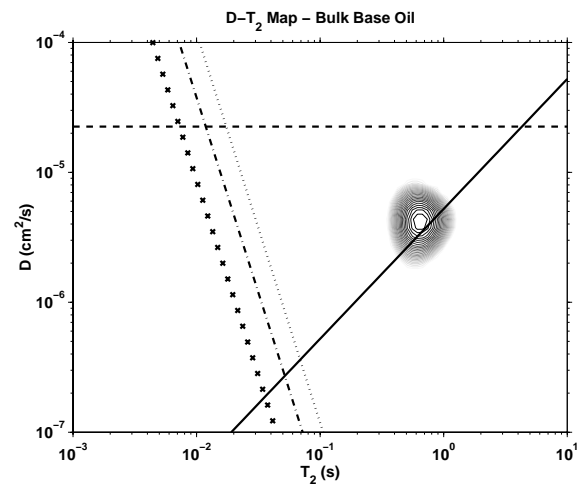


Figure 12: Bulk Base Oil $D - T_2$ Map. The Presence of Surfactant Additives does not effect this map.

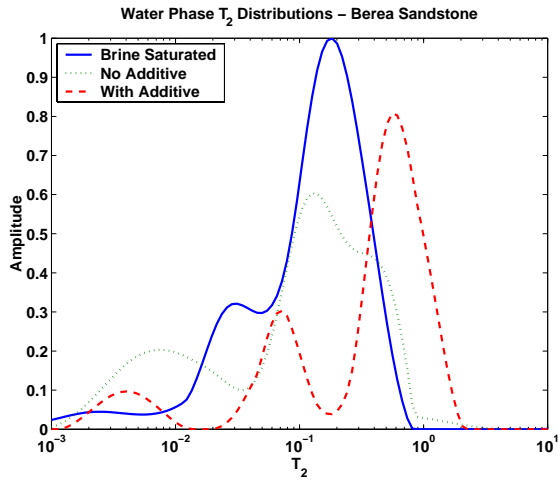


Figure 13: Relaxation Time Distributions for Water Phase in Berea Sandstone

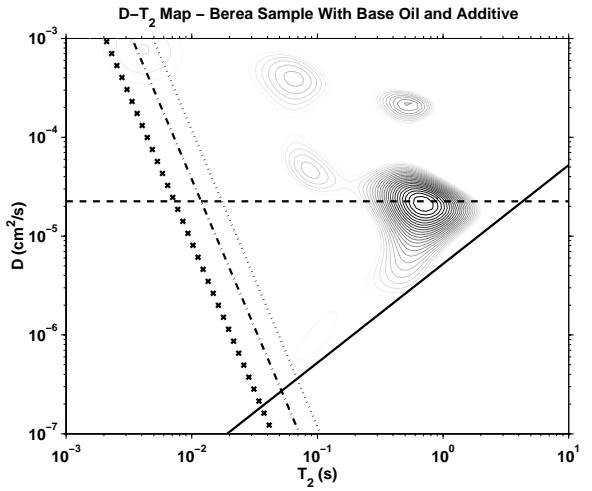


Figure 15: Berea Sandstone $D - T_2$ Map, Partially Saturated With Base Oil, With 3% NOVA Surfactant Additive

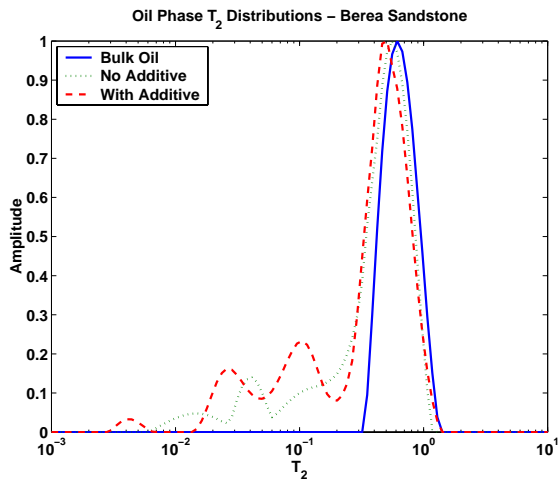


Figure 14: Relaxation Time Distributions for Oil Phase in Berea Sandstone